EUROPEAN JOURNAL OF PURE AND APPLIED MATHEMATICS
2025, Vol. 18, Issue 3, Article Number 6447
ISSN 1307-5543 – ejpam.com
Published by New York Business Global

Analysis of a Smoking Dynamics Model with Age-Dependent Incidence Function

Samia Bushnaq[1], Sameera Bano[2], Anwar Zeb[2,*]

[1] *Department of Basic Sciences, Princess Sumaya University for Technology, Amman 11941, Jordan*
[2] *Department of Mathematics COMSATS University Islamabad, Abbottabad Campus, KPK, Pakistan*

Abstract. Smoking remains a major public health concern, influenced significantly by age structure and household environments. In this study, we develop and analyze an age-structured mathematical model that incorporates age-dependent incidence and household effects to better understand smoking dynamics. We establish the model's well-posedness by proving the existence and uniqueness of solutions. The global stability of both smoking-free and endemic equilibria is analyzed using a suitably constructed Lyapunov function. For numerical simulations, we apply the nonstandard finite difference (NSFD) method and compare the results with those obtained via the classical fourth-order Runge–Kutta (RK4) scheme. The findings underscore the importance of age-specific interventions and offer a framework for future studies incorporating relapse, control strategies, or stochastic effects.

2020 Mathematics Subject Classifications: 92D30, 34D20, 65L12, 37N25

Key Words and Phrases: Age-Structured Smoking Model, Equilibria, Stability Analysis, Lyapunov Function, Non-Standard Finite Difference Technique

1. Introduction

Mathematical modeling has become an indispensable tool in modern epidemiology and public health research. These models have been extensively employed to study a wide range of diseases, including infectious diseases such as influenza, COVID-19, HIV/AIDS, and tuberculosis, as well as non-communicable diseases like cancer, diabetes, and cardiovascular conditions [1–4]. By incorporating biological, environmental, social, and behavioral variables, mathematical models help predict disease dynamics, assess the impact of interventions, and formulate effective public health policies [5–7]. For instance, compartmental models such as SIR and SEIR frameworks have been used to analyze the spread of infectious agents, while more complex models with delays, spatial heterogeneity, and control strategies have been applied to cancer progression, substance abuse, and mental health disorders [8, 9].

In recent years, the scope of mathematical modeling has expanded to behavioral health problems, including tobacco use and smoking. Smoking remains a persistent global health challenge, contributing significantly to mortality and morbidity rates across both developed and developing nations. It is directly linked to multiple life-threatening conditions, including respiratory diseases, stroke, cardiovascular complications, and various forms of cancer. Statistically, a substantial proportion of the adult American population engages in smoking, with prevalence exceeding that of the adult female population [10–12]. Epidemiological studies reveal that

*Corresponding author.
DOI: https://doi.org/10.29020/nybg.ejpam.v18i3.6447

Email addresses: S.Bushnaq@psut.edu.jo (S. Bushnaq), sameera@cuiatd.edu.pk (S. Bano), anwar@cuiatd.edu.pk (A. Zeb)

smokers face a fourteen-fold increase in the mortality risk from cancers of the respiratory and oral systems compared to nonsmokers [13–15].

While healthcare professionals and pharmaceutical researchers are actively striving to combat smoking through cessation programs and drug therapies, mathematicians also play a crucial role by developing analytical models that improve understanding of smoking behaviors and support evidence-based medical interventions. These models help analyze smoking initiation, continuation, cessation, and relapse by integrating behavioral, psychological, and social components into the mathematical framework [16–20].

Traditionally, smoking behavior has been modeled using classical integer-order differential equations [21, 22]. However, recent approaches have employed fractional-order differential equations due to their capability to capture memory and hereditary effects, which are especially relevant for addictive behaviors like smoking [23, 24]. Stochastic models also contribute to a more realistic representation by incorporating randomness and uncertainty, reflecting population-level variability in smoking tendencies.

Additionally, the inclusion of age-structured modeling has gained prominence in the study of both infectious and non-infectious diseases. Age-specific modeling allows researchers to explore differences in susceptibility, behavior, and exposure across age groups, a feature particularly important in smoking dynamics where younger populations exhibit higher vulnerability to addiction.

Motivated by these observations, we propose and study an age-structured smoking model. The model's development and analysis of the endemic and smoking-free equilibrium points come first. The existence and uniqueness of the model solutions are then established. To investigate long-term dynamics, we perform a global stability analysis of the equilibrium states using an appropriate Lyapunov function. Furthermore, we fix the age variable and implement a nonstandard finite difference (NSFD) approach to numerically approximate the model's solutions, which are then compared graphically with those obtained using the classical fourth-order Runge–Kutta (RK4) method via MATLAB simulations.

The remainder of the paper is structured as follows. Section 2 introduces the formulation of the age-structured model and discusses the existence and uniqueness of solutions. Section 3 analyzes the equilibrium points and their local stability. Section 4 presents the global stability results using the Lyapunov method. In Section 5, we employ the NSFD technique for numerical simulations. Finally, Section 6 concludes the paper with key findings.

2. Model Formulation and Mathematical Well-Posedness

We introduce an age-structured smoking model that incorporates household effects, such as school vacations, that influence smoking initiation rates. The model consists of four compartments: susceptible (S), exposed (E), smokers (I), and recovered (R). The system of ordinary differential equations (ODEs) is given by:

$$\begin{cases} \frac{dS}{dt} &= \Lambda - \beta(a,t)SI - \mu S, \\ \frac{dE}{dt} &= \beta(a,t)SI - (\sigma+\mu)E, \\ \frac{dI}{dt} &= \sigma E - (\gamma+\mu)I, \\ \frac{dR}{dt} &= \gamma I - \mu R. \end{cases} \tag{1}$$

Here, Λ is the recruitment rate, μ is the natural death rate, σ is the transition rate from the exposed class to the infected class, γ is the transition rate from the infected class to the recovered class, $\beta(a,t)$ represents the transmission rate, which varies seasonally according to the effect of the household model:

$$\beta(a,t) = \beta_0 \left(1 + \epsilon \cos\left(\frac{2\pi t}{T}\right)\right),$$

where ϵ captures the strength of seasonal effects (e.g., school vacations), and T represents the yearly period. By adding equations from 1-4 of the model (1), we get

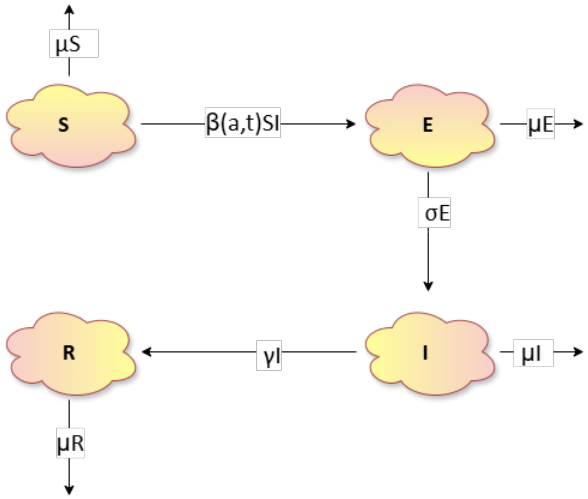

Figure 1: Flow Chart for model (1)

$$\frac{dN}{dt} = \Lambda - \mu N$$

$$\frac{dN}{dt} + \mu N = \Lambda$$

$$\implies N = \frac{\Lambda}{\mu} + \left(N_o - \frac{\Lambda}{\mu}\right)\exp(-\mu t)$$

as $t \to \infty$, we get $N = \frac{\Lambda}{\mu}$, which implies that the given system has a unique solution.

3. Existence of Equilibrium Points

At equilibrium, the time derivatives are zero.
Setting $\frac{dS}{dt} = 0$, $\frac{dE}{dt} = 0$, $\frac{dI}{dt} = 0$, $\frac{dR}{dt} = 0$, the equilibrium equations become

$$\begin{aligned}
\Lambda - \beta(a,t)SI - \mu S &= 0,\\
\beta(a,t)SI - (\sigma + \mu)E &= 0,\\
\sigma E - (\gamma + \mu)I &= 0,\\
\gamma I - \mu R &= 0.
\end{aligned}$$

Solving these equations, we get a smoking-free equilibrium point

$$D_0(S_0, E_0, I_0, R_0),$$

where

$$S_0 = \frac{\Lambda}{\mu}.$$

For an endemic equilibrium point, we have $I > 0$.
The given system has an existence of unique positive equilibrium

$$D_*(S^*, E^*, I^*, R^*),$$

where

$$\begin{aligned} S^* &= \frac{(\sigma+\mu)(\gamma+\mu)}{\beta\sigma}, & E^* &= \frac{\mu(\gamma+\mu)(R_0-1)}{\sigma\beta}, \\ I^* &= \frac{\mu(R_0-1)}{\beta}, & R^* &= \frac{\gamma(R_0-1)}{\beta}. \end{aligned}$$

So there exists an endemic equilibrium point for $R_0 - 1 > 0$.

3.1. Stability and Basic Reproduction Number

The basic reproductive number, R_0, is calculated as the spectral radius of the next-generation matrix:

$$R_0 = \frac{\beta\sigma\lambda}{\mu(\sigma+\mu)(\gamma+\mu)}.$$

3.2. Local Stability Analysis

Theorem 1. *Smoking-free equilibriums are locally asymptotically stable when* $R_0 < 1$.

Proof. The smoking-free equilibrium (SFE) is given by $(S^0, E^0, I^0, R^0) = (\frac{\Lambda}{\mu}, 0, 0, 0)$. The Jacobian matrix evaluated at SFE is as follows:

$$J = \begin{bmatrix} -\mu & 0 & -\beta S^0 & 0 \\ 0 & -(\sigma+\mu) & \beta S^0 & 0 \\ 0 & \sigma & -(\gamma+\mu) & 0 \\ 0 & 0 & \gamma & -\mu \end{bmatrix}. \tag{2}$$

For eigenvalues, we solve $|J - \lambda' I| = 0$,

$$|J - \lambda' I| = \begin{vmatrix} -\mu-\lambda' & 0 & -\beta S^0 & 0 \\ 0 & -(\sigma+\mu)-\lambda' & \beta S^0 & 0 \\ 0 & \sigma & -(\gamma+\mu)-\lambda' & 0 \\ 0 & 0 & \gamma & -\mu-\lambda' \end{vmatrix} = 0.$$

Expanding by C_1

$$(-\mu-\lambda') \begin{vmatrix} -(\sigma+\mu)-\lambda' & \beta S^0 & 0 \\ \sigma & -(\gamma+\mu)-\lambda' & 0 \\ 0 & \gamma & -\mu-\lambda' \end{vmatrix} = 0,$$

again expand with C_1

$$\implies \quad \big(-\mu-\lambda'\big)\Big[\big(-(\sigma+\mu)-\lambda'\big)\Big(\big((\gamma+\mu)+\lambda'\big)(\mu+\lambda')\Big) - \sigma\big(-\beta S^0(\mu+\lambda')\big)\Big] = 0,$$

$$\implies \quad \big(-\mu-\lambda'\big)\Big[\big(-(\sigma+\mu)-\lambda'\big)\Big(\lambda'^2 + \mu\lambda' + \mu(\gamma+\mu) + \lambda'(\gamma+\mu)\Big) + \sigma\beta S^0\mu + \sigma\beta S^0\lambda'\Big] = 0,$$

$$\begin{aligned}\implies \quad & \big(-\mu-\lambda'\big)\bigg(-\lambda'^3-(\gamma+2\mu)\lambda'^2-\mu(\gamma+\mu)\lambda'-(\sigma+\mu)\lambda'^2\\ - \quad & (\sigma+\mu)(\gamma+2\mu)\lambda'-(\sigma+\mu)\mu(\gamma+\mu)+\sigma\beta S^0\mu+\sigma\beta S^0\lambda'\bigg)=0.\end{aligned}$$

Thus, it follows the following equation,

$$\begin{aligned}\implies \quad & \big(-\mu-\lambda'\big)\bigg[\lambda'^3+(\gamma+3\mu+\sigma)\lambda'^2+\big(\mu(\gamma+\mu)+(\sigma+\mu)(\gamma+2\mu)-\beta S^0\sigma\big)\lambda'\\ + \quad & (\sigma+\mu)\mu(\gamma+\mu)-\beta S^0\sigma\mu\bigg]=0,\end{aligned}$$

From the following inequalities:

$$\begin{aligned}\implies \quad & \beta S^0\sigma<(\sigma+\mu)(\gamma+\mu),\\ \implies \quad & \beta S^0\sigma<(\sigma+\mu)(\gamma+2\mu),\end{aligned}$$

it follows that $R_0<1$, which implies that the characteristic equation associated with the linearized system at the smoking-free equilibrium has negative roots.

Moreover, the corresponding characteristic polynomial satisfies the Routh-Hurwitz stability criteria under the condition $R_0<1$. Therefore, all eigenvalues of the Jacobian matrix have negative real parts, confirming that the smoking-free equilibrium is locally asymptotically stable.

Theorem 2. *The positive (endemic) equilibrium is locally asymptotically stable if $R_0>1$.*

Proof. The endemic equilibrium is given by

$$(S^*,E^*,I^*,R^*)=\left(\frac{(\sigma+\mu)(\gamma+\mu)}{\beta\sigma},\frac{\mu(\gamma+\mu)(R_0-1)}{\sigma\beta},\frac{\mu(R_0-1)}{\beta},\frac{\gamma(R_0-1)}{\beta}\right).$$

The Jacobian matrix evaluated at the endemic equilibrium point is

$$J=\begin{bmatrix}-\beta I^*-\mu & 0 & -\beta S^* & 0\\ \beta I^* & -(\sigma+\mu) & \beta S^* & 0\\ 0 & \sigma & -(\gamma+\mu) & 0\\ 0 & 0 & \gamma & -\mu\end{bmatrix}.$$

To determine the eigenvalues, we solve the characteristic equation $|J-\lambda' I|=0$, which becomes

$$|J-\lambda' I|=\begin{bmatrix}-\beta I^*-\mu-\lambda' & 0 & -\beta S^* & 0\\ \beta I^* & -(\sigma+\mu)-\lambda' & \beta S^* & 0\\ 0 & \sigma & -(\gamma+\mu)-\lambda' & 0\\ 0 & 0 & \gamma & -\mu-\lambda'\end{bmatrix}=0.$$

Expanding along the fourth column C_4, we obtain

$$(-\mu-\lambda')\begin{vmatrix}-\beta I^*-\mu-\lambda' & 0 & -\beta S^*\\ \beta I^* & -(\sigma+\mu)-\lambda' & \beta S^*\\ 0 & \sigma & -(\gamma+\mu)-\lambda'\end{vmatrix}=0.$$

This yields one eigenvalue $\lambda'=-\mu$.

Next, we expand the remaining 3×3 determinant along the first column C_1, leading to:

$$\big(-\beta I^*-\mu-\lambda'\big)\bigg(\big((\sigma+\mu)+\lambda'\big)\big((\gamma+\mu)+\lambda'\big)-\beta\sigma S^*\bigg)-\beta^2\sigma I^*S^*=0,$$

$$\big(-\beta I^* - \mu - \lambda'\big)\Big(\lambda'^2 + \big((\sigma+\mu)+(\gamma+\mu)\big)\lambda' + (\sigma+\mu)(\gamma+\mu) - \beta\sigma S^*\Big) - \beta^2\sigma I^* S^* = 0,$$

$$\lambda'^3 + \big((\sigma+\mu)+(\gamma+\mu)+\beta I^*+\mu\big)\lambda'^2 + \Big(\big((\sigma+\mu)(\gamma+\mu) - \beta\sigma S^*\big) + (\beta I^*+\mu)\big((\sigma+\mu)+(\gamma+\mu)\big)\Big)\lambda'$$
$$+(\beta I^*+\mu)\big((\sigma+\mu)(\gamma+\mu) - \beta\sigma S^*\big) + \beta^2\sigma I^* S^* = 0.$$

Given that

$$S^* = \frac{(\sigma+\mu)(\gamma+\mu)}{\beta\sigma},$$

the above equation simplifies to the reduced form:

$$\lambda'^3 + \big(\sigma + 3\mu + \gamma + \beta I^*\big)\lambda'^2 + (\beta I^*+\mu)\big(\sigma + 2\mu + \gamma\big)\lambda' + \beta^2\sigma I^* S^* = 0,$$

where

$$I^* = \frac{\mu(R_0-1)}{\beta}, \quad \text{for } R_0 > 1.$$

Since all the coefficients of the above cubic polynomial are positive for $R_0 > 1$, the Routh–Hurwitz criteria are satisfied. Therefore, all roots of the characteristic equation have negative real parts. This confirms that the endemic equilibrium is locally asymptotically stable.

4. Global Stability Analysis Using Lyapunov Function

4.1. Smoking-Free Equilibrium Point

Theorem 3. *Smoking-free equilibrium point is globally asymptotically stable for $R_0 < 1$.*

Proof. To show global stability at smoking-free equilibrium point, we build a Lyapunov function:

$$V = \int_0^A (\frac{E^2}{2} + \frac{I^2}{2})da. \tag{3}$$

This function is
1) positive definite, i-e $V(t) > 0$, when $E = I = 0$.
2) Zero only at the equilibrium point $E = I = 0$.
3) Differentiable in time.

Taking the time derivative:

$$\frac{dV}{dt} = \int_0^A (E\frac{dE}{dT} + I\frac{dI}{dt})da.$$

By substituting the model (1) equations, we get

$$\frac{dV}{dt} = \int_0^A \Big(E\big(\beta SI - (\sigma+\mu)E\big) + I\big(\sigma E - (\gamma+\mu)I\big)\Big)da,$$

$$\frac{dV}{dt} = \int_0^A \Big(\beta(a,t)SEI - (\sigma+\mu)E^2 + \sigma EI - (\gamma+\mu)I^2\Big)da,$$

$$\frac{dV}{dt} = \int_0^A \Big(\lambda(a,t)SE + \sigma EI - (\sigma+\mu)E^2 - (\gamma+\mu)I^2\Big)da,$$

where $\lambda = \beta(a,t)I$

$$\frac{dV}{dt} = -\int_0^A ((\sigma+\mu)E^2 + (\gamma+\mu)I^2)da + \int_0^A (\lambda(a,t)SE + \sigma EIda).$$

Now, we analyze the sign of $\frac{dV}{dt}$. Using Young's inequality $ab \leq \frac{a^2}{2} + \frac{b^2}{2}$ for cross terms.

$$\lambda SE \leq \frac{\lambda^2 S^2}{2\epsilon_1} + \frac{\epsilon_1 E^2}{2},$$

and

$$\sigma EI \leq \frac{\sigma^2 E^2}{2\epsilon_2} + \frac{\epsilon_2 I^2}{2}.$$

So

$$\frac{dV}{dt} \leq -\int_0^A ((\sigma+\mu)E^2 + (\gamma+\mu)I^2)da + \int_0^A \left(\frac{\lambda^2 S^2}{2\epsilon_1} + \frac{\epsilon_1 E^2}{2} + \frac{\sigma^2 E^2}{2\epsilon_2} + \frac{\epsilon_2 I^2}{2}\right)da.$$

By rearranging

$$\frac{dV}{dt} \leq -\int_0^A \big(\big(\sigma+\mu-\frac{\epsilon_1}{2}-\frac{\sigma^2}{2\epsilon_2}\big)E^2 - \big(\gamma+\mu-\frac{\epsilon_2}{2}\big)I^2\big)da + \int_0^A \frac{\lambda^2 S^2}{2\epsilon_1}da.$$

If smoking prevalence is small,
i-e λ is small,
i-e $\lambda(t) \to 0$ as $I(t) \to 0$,
then $\lambda^2 S^2$ is small near the equilibrium point, so the last term of the above equation is negligible.
Choose ϵ_1, ϵ_2 such that

$$\sigma - \frac{\epsilon_1}{2} - \frac{\sigma^2}{2\epsilon_2} > 0,$$

and

$$\gamma - \frac{\epsilon_2}{2} > 0,$$

then $\frac{dV}{dt} \leq 0$.
The equality holds only when $E = I = 0$.
According to Lasalle's principle of invariance, the smoking-free equilibrium point is globally asymptotically stable.

4.2. Positive Equilibrium point

Theorem 4. *Positive equilibrium point is globally asymptotically stable.*

Proof. To show the global stability of the endemic equilibrium point, we construct a Lyapunov function

$$V(t) = \frac{1}{2}(E-E^*)^2 + \frac{1}{2}(I-I^*)^2,$$

$$\implies \frac{dV}{dt} = (E-E^*)\frac{dE}{dt} + (I-I^*)\frac{dI}{dt}.$$

From the model (1) equations

$$\frac{dE}{dt} = \beta SI - (\sigma+\mu)E,$$

and

$$\frac{dI}{dt} = \sigma E - (\gamma+\mu)I,$$

$$\implies \frac{dV}{dt} = (E-E^*)\big(\beta SI - (\sigma+\mu)E\big) + (I-I^*)\big(\sigma E - (\gamma+\mu)I\big),$$

$$\implies \tfrac{dV}{dt} = (E-E^*)\big((\sigma+\mu)E^* - (\sigma+\mu)E\big) + (E-E^*)(\beta SI - \beta S^* I^*)$$

$$+(I-I^*)(\sigma E-\sigma E^*)+(I-I^*)\big((\gamma+\mu)I^*-(\gamma+\mu)I\big),$$

$$\implies \tfrac{dV}{dt}=-(\sigma+\mu)(E-E^*)^2+(E-E^*)(\beta SI-\beta S^*I^*)+\sigma(I-I^*)(E-E^*)-(I-I^*)^2(\gamma+\mu),$$

$$\implies \frac{dV}{dt}=-(\sigma+\mu)(E-E^*)^2-(I-I^*)^2(\gamma+\mu)+(E-E^*)(\beta SI-\beta S^*I^*)+\sigma(I-I^*)(E-E^*).$$

Use Young's inequality on cross terms, we have

$$(E-E^*)(I-I^*)\leq\frac{1}{2}(E-E^*)^2+\frac{1}{2}(I-I^*)^2,$$

and

$$(E-E^*)(\lambda S-\lambda^*S)\leq\frac{1}{2\epsilon}(\lambda S-\lambda^*S^*)^2+\frac{\epsilon}{2}(E-E^*)^2.$$

Thus we can bound $\frac{dV}{dt}$ by

$$\begin{aligned}\tfrac{dV}{dt}\leq&-(\sigma+\mu)(E-E^*)^2-(I-I^*)^2(\gamma+\mu)+\tfrac{1}{2\epsilon}(\lambda S-\lambda^*S^*)^2\\&+\tfrac{\sigma}{2}(E-E^*)^2+\tfrac{\sigma}{2}(I-I^*)^2,\end{aligned}$$

$$\implies \frac{dV}{dt}\leq-(\frac{\sigma}{2}+\mu)(E-E^*)^2-(\gamma+\mu-\frac{\sigma}{2})(I-I^*)^2+\frac{1}{2\epsilon}(\lambda S-\lambda^*S^*)^2.$$

If $(\lambda S-\lambda^*S^*)$ is small near the equilibrium and if the parameters satisfy $\gamma+\mu>\frac{\sigma}{2}$, then $\frac{dV}{dt}<0$ near the equilibrium. This implies global asymptotic stability of the endemic equilibrium.

5. Numerical Simulations

We solve the system numerically using non-standard MATLAB, employing the Euler method and varying $\beta(a,t)$ to simulate household effects. The results illustrate the impact of seasonal variations on the prevalence. The initial conditions are E(0)=50, I(0)=30, R(0)=20 and P(0)=N-E(0)-I(0)-R(0). Parameters values are given in below table;

Parameter	values
Λ	10.25
β_0	0.005
σ	0.1
γ	0.03
ϵ	0,05
N	250

Table 1: Parameter values for the proposed model

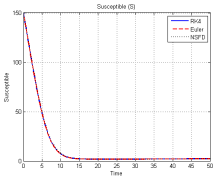

(a) Comparison of Susceptible population with RK4, Euler, Nonstandard finite difference method

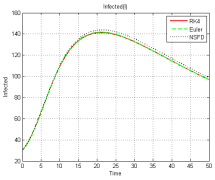

(b) Comparison of exposed population with RK4, Euler, Nonstandard finite difference method

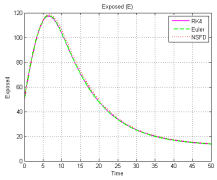

(c) Comparison of infected population with RK4, Euler, Nonstandard finite difference method

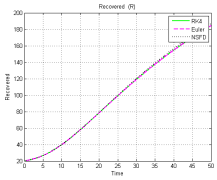

(d) Comparison od recovered population with RK4,Euler, Nonstandard finite difference method

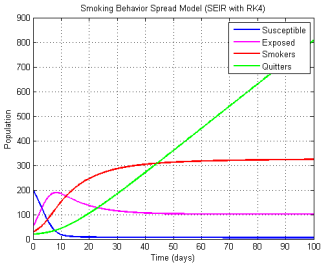

(e) population graph with RK4

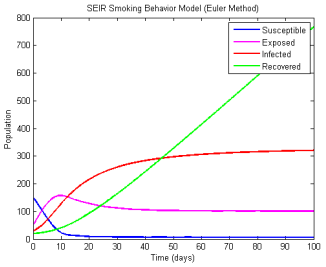

(f) Population graph with Euler

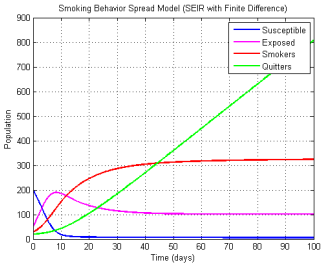

(g) Population graph with NSFD

Figure 2: (a) plot of susceptible class in which RK4, Euler and Nonstandard finite difference. (b) plot of infected class in which RK4, Euler and Nonstandard finite difference. (c) plot of exposed class in which RK4, Euler and Nonstandard finite difference. (d) plot of recovered class in which RK4, Euler and Nonstandard finite difference (e) plot of population with RK4 method. (e) plot of population with Euler method. (f) plot of population with nonstandard finite difference method.

For different value of $b(a,t)$ the graph of all population by using RK4, Euler, and nonstandard finite difference method are given below.

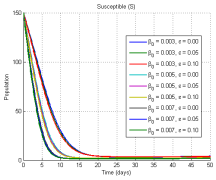

(a) Susceptible population using the RK4 technique with various numbers of $\beta(a,t)$

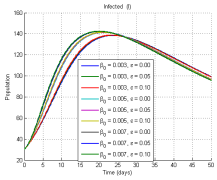

(b) Infected population using the RK4 technique with various numbers of $\beta(a,t)$

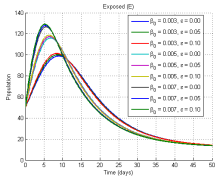

(c) Exposed population using the RK4 technique with various numbers of $\beta(a,t)$

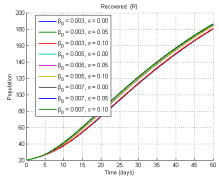

(d) Recovered population using the RK4 technique with various numbers of $\beta(a,t)$

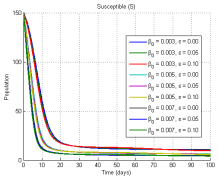

(e) Susceptible population using the Euler technique with various numbers of $\beta(a,t)$

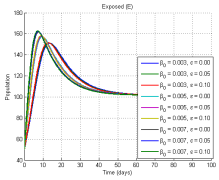

(f) Exposed population using the Euler technique with various numbers of $\beta(a,t)$

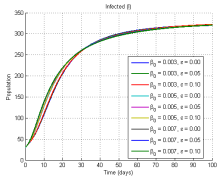

(g) Infected population using the Euler technique with various numbers of $\beta(a,t)$

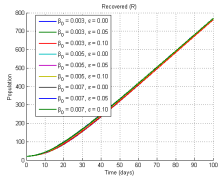

(h) Recovered population using the Euler technique with various numbers of $\beta(a,t)$

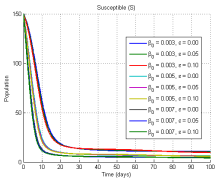

(i) Susceptible population using the NSFD technique with various numbers of $\beta(a,t)$

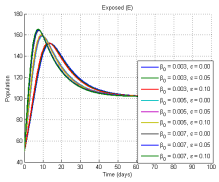

(j) Exposed population using the NSFD technique with various numbers of $\beta(a,t)$

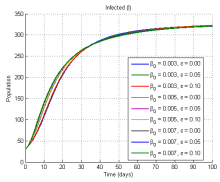

(k) Infected population using the NSFD technique with various numbers of $\beta(a,t)$

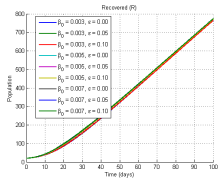

(l) Recovered population using the NSFD technique with various numbers of $\beta(a,t)$

Figure 3: (a) plot of susceptible class in which RK4 method is used for different value of $\beta(a,t)$. (b)plot of exposed class in which RK4 method is used for different value of $\beta(a,t)$. (c) plot of infected class in which RK4 method is used for different value of $\beta(a,t)$ (d) plot of recovered class in which RK4 method is used for different value of $\beta(a,t)$. (e) plot of susceptible class in which Euler method is used for different value of $\beta(a,t)$. (f) plot of exposed class in which Euler method is used for different value of $\beta(a,t)$. (g) plot of infected class in which Euler method is used for different value of $\beta(a,t)$. (h) plot of recovered class in which Euler method is used for different value of $\beta(a,t)$. (i) plot of susceptible class in which nonstandard finite difference method is used for different value of $\beta(a,t)$.(j) plot of exposed class in which nonstandard finite difference method is used for different value of $\beta(a,t)$. (k) plot of infected class in which nonstandard finite difference method is used for different value of $\beta(a,t)$.(l) plot of recovered class in which nonstandard finite difference method is used for different value of $\beta(a,t)$.

6. Conclusions and Discussions

The current paper investigated the global asymptotic dynamics of an age-structured smoking model. Our initial step involved formulating the model and verifying that it admits a unique solution. We then analyzed the equilibrium points, including the smoking-free and endemic equilibria. To establish the global asymptotic stability of these points, we constructed an appropriate Lyapunov function. The analytical results were supported by numerical simulations,

which validated the model behavior for different parameter values. The impact of the incremental rate was examined through graphical results, highlighting the sensitivity of the model to behavioral transitions across age groups.

Compared to previous models in the literature, our age-structured formulation adds a significant layer of realism, especially in modeling differential susceptibility and recovery rates among distinct age cohorts. This provides a refined framework for analyzing the spread and persistence of smoking behaviors in populations.

In line with the reviewer's recommendation, this work opens several promising avenues for future research. One natural extension is to incorporate **relapse dynamics**, allowing former smokers to return to smoking under certain behavioral or social conditions. Moreover, integrating **intervention strategies**, such as public health campaigns or medical treatments, could enhance the practical relevance of the model. Additionally, the inclusion of **stochastic effects** would enable the modeling of randomness and uncertainty in smoking behaviors and policy outcomes, which is particularly important for small populations or individual-level modeling. These enhancements can lead to more comprehensive insights and provide policymakers with robust tools to design targeted anti-smoking strategies.

References

[1] R. M. Anderson and R. M. May. *Infectious Diseases of Humans: Dynamics and Control*. Oxford University Press, 1991.

[2] H. W. Hethcote. The mathematics of infectious diseases. *SIAM Review*, 42(4):599–653, 2000.

[3] F. Brauer, C. Castillo-Chavez, and Z. Feng. *Mathematical Models in Epidemiology*. Springer, 2019.

[4] O. Diekmann, J. A. P. Heesterbeek, and T. Britton. *Mathematical Tools for Understanding Infectious Disease Dynamics*. Princeton University Press, 2013.

[5] L. G. de Pillis and A. E. Radunskaya. A mathematical tumor model with immune resistance and drug therapy: an optimal control approach. *Journal of Theoretical Biology*, 238(4):841–862, 2006.

[6] M. Gümüs and Ö. Öcalan. Global asymptotic stability of a nonautonomous difference equation. *Journal of Applied Mathematics*, 2014:Article ID 395954, 5 pages, 2014.

[7] M. Y. Li and J. S. Muldowney. Global stability for the seir model in epidemiology. *Mathematical Biosciences*, 125(2):155–164, 1995.

[8] J. Wang, M. Zhang, and W. Yang. Dynamics and asymptotic profiles of a local-nonlocal dispersal sir epidemic model with spatial heterogeneity. *Journal of Differential Equations*, 313:1–34, 2022.

[9] C. Liu and J. Shi. Traveling wave solution for a delayed reaction-diffusion two-group sir epidemic model with a generalized nonlinear incidence function. *Nonlinear Analysis: Real World Applications*, 65:103434, 2022.

[10] E. Alzahrani and A. Zeb. Stability analysis and prevention strategies of tobacco smoking model. *Boundary Value Problems*, 2020:1–13, 2020.

[11] A. Zeb, S. Kumar, A. Tesfay, and A. Kumar. A stability analysis on a smoking model with stochastic perturbation. *International Journal of Numerical Methods for Heat and Fluid Flow*, 32(3):915–930, 2022.

[12] S. M. Lestari, Y. Yulida, A. S. Lestia, and M. A. Karim. Stability analysis of a smoking behavior model. *Journal of Physics: Conference Series*, 2106(1):012025, 2021.

[13] A. M. Pulecio-Montoya, L. E. López-Montenegro, and L. M. Benavides. Analysis of a mathematical model of smoking. *Contemporary Engineering Sciences*, 12(3):117–129, 2019.

[14] Z. Alkhudari, S. Al-Sheikh, and S. Al-Tuwairqi. The effect of occasional smokers on the dynamics of a smoking model. *International Mathematical Forum*, 9(25):1207–1222, 2014.

[15] G. Zaman and S. Gul. Qualitative behavior of giving up smoking models. *Bulletin of the Malaysian Mathematical Sciences Society. Second Series*, 34(2):403–415, 2011.

[16] Z. Alkhudhari, S. Al-Sheikh, and S. Al-Tuwairqi. Global dynamics of a mathematical model on smoking. *International Scholarly Research Notices*, 2014(1):847075, 2014.

[17] A. Zeb, G. Zaman, S. Momani, and S. Shaher. Square-root dynamics of a giving up smoking model. *Applied Mathematical Modelling*, 37(7):5326–5334, 2013.

[18] A. Zeb, A. Bano, E. Alzahrani, and G. Zaman. Dynamical analysis of cigarette smoking model with a saturated incidence rate. *AIP Advances*, 8(4), 2018.

[19] Y. S. Tan, X. X. Li, J. Yang, and R. A. Cheke. Global stability of an age-structured model of smoking and its treatment. *International Journal of Biomathematics*, 16(01):2250063, 2023.

[20] A. Zeb, S. Hussain, O. J. Algahtani, and G. Zaman. Global aspects of age-structured cigarette smoking model. *Mediterranean Journal of Mathematics*, 15:1–11, 2018.

[21] E. Addai, A. Adeniji, O. J. Peter, J. O. Agbaje, and K. Oshinubi. Dynamics of age-structure smoking models with government intervention coverage under fractal-fractional order derivatives. *Fractal and Fractional*, 7(5):370, 2023.

[22] S. Djilali, S. Bentout, A. Zeb, S. Saeed, and T. Tareq. Global stability of hybrid smoking model with nonlocal diffusion. *Fractals*, 30(08):2240224, 2022.

[23] A. Lahrouz, L. Omari, D. Kiouach, and A. Belmaâti. Deterministic and stochastic stability of a mathematical model of smoking. *Statistics & Probability Letters*, 81(8):1276–1284, 2011.

[24] A. Zeb, G. Zaman, I. H. Jung, and M. Khan. Optimal campaign strategies in fractional-order smoking dynamics. *Zeitschrift für Naturforschung A*, 69(5-6):225–231, 2014.